

Review

# Circularly Polarized Hybrid Dielectric Resonator Antennas: A Brief Review and Perspective Analysis

Rajasekhar Nalanagula <sup>1</sup>, Naresh K. Darimireddy <sup>2,\*</sup> , Runa Kumari <sup>1</sup>, Chan-Wang Park <sup>2</sup> and R. Ramana Reddy <sup>3</sup>

<sup>1</sup> Department of Electrical and Electronics Engineering, BITS-Pilani, Hyderabad 500078, India; rajasekhar434@gmail.com (R.N.); runakumari@hyderabad.bits-pilani.ac.in (R.K.)

<sup>2</sup> Department of Mathematics, Computer Science and Engineering, University of Quebec, Rimouski, QC G5L 3A1, Canada; chanwang\_park@uqar.ca

<sup>3</sup> Department of Electronics and Communication Engineering, JNTUA College of Engineering Pulivendula, Andhra Pradesh 516390, India; profrrreddy@yahoo.co.in

\* Correspondence: darn0005@uqar.ca

**Abstract:** Recently, it has been a feasible approach to build an antenna, in view of the potential advantages they offer. One of the recent trends in dielectric resonator antenna research is the use of compound and hybrid structures. Several considerable investigations have been already underway showing quite interesting and significant features in bandwidth, gain, and generation of circular polarization. A critical review on a journey of circularly polarized hybrid dielectric resonator antennas is presented in this article. A general discussion of circular polarization and DR antennas are provided at the forefront. Evolution, significant challenges, and future aspects with new ideas in designing hybrid dielectric resonator antennas are indicated at the end of the review. State-of-the-art advances and associated design challenges of circularly polarized hybrid DR antennas and related empirical formulas used to find resonance frequency of different hybrid modes produced are discussed in this paper.

**Keywords:** CP radiation; microstrip antenna; dielectric-resonator antenna; hybrid dielectric resonator antenna; wide-band antennas; multi-functional antennas



**Citation:** Nalanagula, R.; Darimireddy, N.K.; Kumari, R.; Park, C.-W.; Reddy, R.R. Circularly Polarized Hybrid Dielectric Resonator Antennas: A Brief Review and Perspective Analysis. *Sensors* **2021**, *21*, 4100. <https://doi.org/10.3390/s21124100>

Academic Editors: Halim Boutayeb, Divitha Seetharamdoo and Antonio Lázaro

Received: 18 March 2021

Accepted: 8 June 2021

Published: 15 June 2021

**Publisher's Note:** MDPI stays neutral with regard to jurisdictional claims in published maps and institutional affiliations.



**Copyright:** © 2021 by the authors. Licensee MDPI, Basel, Switzerland. This article is an open access article distributed under the terms and conditions of the Creative Commons Attribution (CC BY) license (<https://creativecommons.org/licenses/by/4.0/>).

## 1. Introduction

The radiation mechanism of various types of antennas and their radiation fundamentals, focusing on the concepts of circular polarization, are comprehensively discussed in [1,2]. Circularly polarized (CP) antennas can offer a consistent or reliable system connection between the transmitter and receiver, since the polarization of the antennas is always associated. In and around the intended resonant frequency, two modes orthogonal to each other with a phase-shift of  $90^\circ$  are desired for circular polarization. Sometimes, the horizontal and vertical field components of a communications link are highly uncorrelated. Therefore, using receiver antennas with the same phase center and orthogonal polarizations can avoid location-induced phase variation.

Generally, a circularly polarized antenna should have the following essential characteristics,

- Nearly equal magnitudes for two orthogonal modes or polarizations and equal radiation pattern shapes.
- Nearly  $\pm 90^\circ$  difference in phase over a wide-bandwidth and wide-beam width.
- Small axial ratio (close to 0 dB i.e.,  $< 3$  dB or numerical 1) over a wide-AR bandwidth and wide-beam width.

The polarization of a wave is expressed in terms of the figure traced as a function of time by the extremity of the E-field vector at a fixed location in space, the sense in which it

is traced, and observed along the direction of propagation. The instantaneous electric field of a uniform plane wave pointed in the negative z-axis is expressed by Equation (1):

$$\mathbf{E}_i(z, t) = E_{ix}(z, t)\mathbf{a}_x + E_{iy}(z, t)\mathbf{a}_y \quad (1)$$

The instantaneous E-field components of  $x$  and  $y$  are correlated to their complex quantities by the following Equations (2) and (3):

$$E_{ix}(z, t) = E_{ix} \cos(\omega t + \beta z + \Phi_{ix})\mathbf{a}_x \quad (2)$$

and

$$E_{iy}(z, t) = E_{iy} \cos(\omega t + \beta z + \Phi_{iy})\mathbf{a}_y \quad (3)$$

The  $E_{ix}$  and  $E_{iy}$  are amplitudes, and  $\Phi_{ix}$  and  $\Phi_{iy}$  are the corresponding phases in  $x$  and  $y$  directions respectively,  $\omega$  is the angular frequency and  $\beta$  is the propagation constant.

- For linearly polarized (LP) plane wave, the difference of phase angle between the  $x$  and  $y$  components must be:

$$\delta\Phi = \Phi_{iy} - \Phi_{ix} = m\pi, \text{ where } m = 0, 1, 2, \dots \quad (4)$$

- For the circularly polarized wave, the magnitudes of the  $x$  and  $y$  components are equal (i.e.,  $E_{ix} = E_{iy}$ ), and difference in phase angle is odd multiples of  $90^\circ$ , and it is mathematically expressed as:

$$\delta\Phi = \Phi_{iy} - \Phi_{ix} = \begin{cases} +(2m\pi + \frac{\pi}{2}) \text{ for Right Hand CP} \\ \text{or} \\ -(2m\pi + \frac{\pi}{2}) \text{ for Left Hand CP} \end{cases} \quad (5)$$

- If  $\delta\Phi$  does not satisfy Equation (1) or  $E_{ix} \neq E_{iy}$  then the wave is elliptically polarized.

In this review article, conditions for CP radiation, different methods of generating circular polarization in dielectric resonator antennas are studied and analyzed by considering a few standard articles in the open literature. Historical study of microstrip and dielectric resonator-based antennas; the important milestones and significant features of dielectric resonator antennas are discussed and reviewed respectively in Section 2. Various aspects and techniques involved in generating circularly polarized radiation for DR-based antennas are studied, in order to recognize the associated challenges. Consequently, the evolution of dielectric resonator-based hybrid antennas with CP radiation techniques is reviewed comprehensively in Section 3. This article's intention and primary focus are on various design perspectives and the progress of circularly polarized hybrid dielectric resonator antennas.

## 2. Historical Review of DR Antennas and CP Methods

Even though Deschamps was the first to introduce the concept of low-profile microstrip radiators in 1953 [3], it was after 20 years that the original patch antenna was practically developed by Munson [4,5] i.e., in the year 1974. The numerous benefits of microstrip antenna, such as less weight, low volume, easy to integrate with the printed circuit board (PCB) technology, are explored to design different patch configurations and feed mechanisms for numerous applications [6–10]. In today's modern world, the essential need and demand for low-profile and compact antennas to integrate with mobile and personal communication devices has drawn the patch antennas to the forefront.

The radiation mechanism of DRAs is quite different from microstrip radiators with similar excitation methods. The electromagnetic energy fed to the DR is confined to the dielectric material, and the radiating mode of that material is excited, to act as a resonator. In another way, the confined EM energy is controlled through the design of DR, and the energy leaks from the resonator. A wide range of dielectric constants, starting from 8 to over 100 are used. The potential of DRAs was its high-frequency operation and

wide impedance bandwidth with sufficient gain, compared to the metallic patch antennas. Several modes are excited in DRA, similar to the short magnetic or electric dipole antenna radiation patterns. The cause for radiation in the microstrip antenna is the two narrow radiating edges, while the DRA radiates through the entire DR external surface, excluding the grounded area. The reduction of surface-waves is an important advantage of the DRA in conjunction with a patch antenna. However, excitation schemes of the DRA and patch antennas are quite similar, and the behavior of both is similar to that of resonant cavities. The dielectric wavelength is lesser than the free-space wavelength by an element of  $1/\sqrt{(\epsilon_r)}$ , so increasing  $\epsilon_r$  both of them can be made smaller.

Additionally, all the feeding methods used for the patch antenna can also be applied for the DRA. The dimensions of a DRA are of the order  $\lambda_0/\sqrt{(\epsilon_r)}$  or less, where  $\lambda_0$  is the free space wavelength, and  $\epsilon_r$  is the material dielectric-constant. The radiation Q-factor and frequency of resonance can be altered by the aspect ratio of the DRA for a fixed value of  $\epsilon_r$ . With the absence of surface waves, the conductor losses are minimum in DRA and high radiation efficiency can be achieved [11]. Generally, DR is mostly used in traditional applications such as microwave circuits, oscillators and filters [12]. The DR was typically considered as an energy storage element instead of an antenna or radiator [13,14]. Even though Richtmyer first proposed the radiation concept of Dielectric Resonators in 1939, the systematic study and experimentation were carried out by Professor S. A. Long in 1983. Many communication systems' frequency range of interest had increasingly advanced to the near-millimeter and millimeter frequency range (100–300 GHz). The conductor loss at this frequency range for microstrip antennas becomes high, and it yields a reduction in the efficiency of the radiators. After the cylindrical DRA, Long and his colleagues subsequently investigated the rectangular [15], cylindrical [16], and hemispherical [17] DRAs. Other shapes are also investigated, comprising the triangular [18], spherical-cap [19], cylindrical-ring [20], and mushroom-shaped [21] DRAs. Consequently, few review papers are reported in the open literature focusing on various aspects, such as general design equations of DRAs for bandwidth, frequency, and equivalent mode theory [22], study of broadband DRAs [23], design advances in dielectric resonator-based ultra-wideband monopole antennas [24], a historic study of DRAs and its state-of-the-art based on the radiation parameters [25–27], circularly polarized DRAs [28], modeling DRAs using numerical methods [29], application-oriented DRAs [30], various CP methods in DRAs [31], improvement of impedance bandwidth in DRAs [32], and design advances in various types of CP antennas [33].

A few glimpses of circularly polarized DR antennas are studied to acknowledge the design aspects responsible for CP radiation. A pair of orthogonal  $HE_{11\delta}$  modes of a cylindrical ring DRA in phase-quadrature is presented for CP radiation. Mongia et al. reported a DRA with a 3 dB AR (Axial Ratio) beamwidth of 1000 and a minimum AR value of 0.5 dB [34]. A single point probe-fed elliptic DRA is presented for CP radiation with wideband properties and it provides 3.5% of CP bandwidth and 14% of RL bandwidth [35]. A parasitic strip is placed on the adjacent wall of the dielectric resonator to stimulate degenerated modes using finite difference time domain (FDTD) analysis to address the linear and circular polarized modes [36]. A new comb-shaped CP-DRA [37] is proposed, and it offers about 4% AR bandwidth with a gain of 3.5 dBi. A quadruple strip-fed cylindrical DRA using two orthogonal hybrid couplers reported for wideband circular polarization applications [38]. The circularly polarized C-shaped DRA [39] has 19% of AR bandwidth and is enhanced to 50% using a short-circuit microstrip. A compact wideband rectangular DRA based on perforations and edge grounding is investigated in [40]. To reduce the Q-factor (i.e., inversely proportional to bandwidth), square slots (perforations) are bored equivalently all across the DRA. The overall occupancy of DRA is reduced by cutting slots and an edge grounding technique in rectangular DRA. A wideband dual segmented DRA is proposed for X-band applications. An S-shaped slot is used to couple the DR elements, and it offers 37.5% (7.66 to 11.2 GHz) fractional bandwidth with a peak gain of 6 dBi [41]. A wideband CP pixelated DRA is analyzed using a real-coded

genetic algorithm (GA), and it is coupled through a narrow slot on the ground plane [42]. A combination of an L-shaped microstrip line and a conformal strip is used as feed to excite two orthogonal modes in two cubical DR elements for CP radiation and wideband applications [43]. A combination of two L-shaped slots is used for two configurations to obtain dual-sense polarized triband and quadband DR antennas [44] for multi-functional applications. Two wideband cylindrical DR antennas loaded on two configurations of phase delay lines (PDL) are presented [45] for CP radiation at 2.4 GHz applications. The CP radiation with two orthogonal modes is possible due to stub-loaded  $90^\circ$  and  $180^\circ$  PDLs. The wide impedance bandwidth and low spurious feed radiation with minimized surface wave losses are advantages of DRA compared to patch antennas. The requirement of DRAs with wide AR bandwidth and wide impedance bandwidth is increasing day-to-day.

### 3. Classification and Progress of Dielectric Antennas

In defining the radiation properties of various types of dielectric antennas, shape and relative permittivity of dielectric material are the significant parameters [46–50], which add up a degree of freedom compared to microstrip radiators. A Venn diagram based on technological advancements in the field of dielectric antennas is presented in Figure 1.

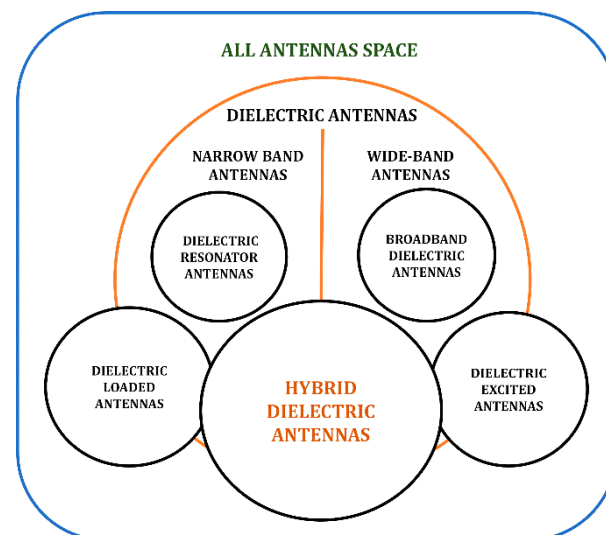


**Figure 1.** Venn Diagram representation for dielectric antenna technology.

The past review studies of the dielectric resonator antennas have been summarized in Table 1 to highlight the various significant radiation and design aspects. The stored energy inside the dielectric is exceptionally high and it is difficult for external objects to detune the device [51–53]. DR can radiate from all surfaces, rendering high radiation efficiency and low Q-factor. Since its birth in the early 1980s, there has been a steady research progress in this area over the years. The bandwidth of a resonant device is a function of its loaded Q, which is controlled by the way of energy, is coupled in and out of the resonant device is under the designer’s control. The unloaded Q is a measure of the internal losses in the device. A device with a high unloaded Q may be used to create an antenna structure with low loaded Q and wide impedance bandwidth. Broadband dielectric antennas can be obtained by suitably configuring the feed structure [54–56].

**Table 1.** Past review highlights of dielectric antennas.

Year	Past Review Highlights	Reference
1994	<ul style="list-style-type: none"> <li>• A detailed review of modes and various radiation parameters of DRAs of different shapes are discussed.</li> <li>• A precise closed-form equation is presented to obtain fundamental resonant frequencies and bandwidth of a cylindrical DR.</li> </ul>	[22]
2005	<ul style="list-style-type: none"> <li>• A brief review of broadband DRAs and design techniques for obtaining multi-resonant frequencies and how these can be combined to form broadband are discussed.</li> </ul>	[23]
2006	<ul style="list-style-type: none"> <li>• Advancements and challenges in designing composite and hybrid dielectric resonator antennas are addressed.</li> </ul>	[41]
2010	<ul style="list-style-type: none"> <li>• A detailed review of various types of monopole-based DR antennas and design methodologies are addressed for ultra-wideband applications.</li> </ul>	[24]
2010	<ul style="list-style-type: none"> <li>• A comprehensive study of history and state-of-the-art design techniques in dielectric resonator antennas over the last 30 years are discussed.</li> </ul>	[25]
2012	<ul style="list-style-type: none"> <li>• A study of recent developments of DR antennas for different radiation parameters and the use of decorative glass blocks as DR elements are presented.</li> </ul>	[26]
2014	<ul style="list-style-type: none"> <li>• Latest developments in the design of dielectric resonator antennas in wideband, multi-band, and ultra-wideband categories have been addressed comprehensively.</li> </ul>	[27]
2015	<ul style="list-style-type: none"> <li>• Various design and developments in methods of CP DRAs are addressed</li> </ul>	[28]
2016	<ul style="list-style-type: none"> <li>• A review of numerical methods used to model the DR elements considering all the effective parameters and characteristics of dielectric antennas</li> </ul>	[29]
2017	<ul style="list-style-type: none"> <li>• An application-oriented detailed survey of DR antennas in the last three and half decades is addressed.</li> </ul>	[30]
2017	<ul style="list-style-type: none"> <li>• A survey of various CP radiation methods for DR antennas is comprehensively discussed.</li> </ul>	[31]
2019	<ul style="list-style-type: none"> <li>• A review of bandwidth improvement methods is highlighted and discussed in detail.</li> </ul>	[32]
2020	<ul style="list-style-type: none"> <li>• Design advances and trends in various types of CP antennas are studied comprehensively</li> </ul>	[33]

The primary radiating component of the *Dielectric Loaded Antennas* is a conducting element and the dielectric modifies the medium, imparting significant performance advantages [57–61]. Dielectric antennas can be used to excite parasitic copper antennas or vice versa. In this class of antennas, often the conductor forms the major radiating part of the antenna. There are bandwidth advantages in this dielectric–copper hybrid approach of the *Dielectric Excited Antennas* [62–65]. Dielectric resonator-based loaded antennas and excited antennas come under the category of *Hybrid Dielectric Resonator Antennas*. Mongia et al. introduced a combination of the grounded metallic post at the center of cylindrical DR elements to produce the lowest order mode for which the overall size of the DRA has been significantly reduced [66].

Similarly, the frequency shift is also possible with the circular metallic disk on the top of the DR element, either isolated or grounded using metallic posts reported by Li et al. [67]. A combination of monopole and ring-shaped DRA forming hybrid structures [68] is developed for ultra-wideband applications with omnidirectional patterns. Further, a microstrip loaded with small cylindrical DRA combination with a wide impedance bandwidth of 10% is reported [69], compared to microstrip alone. Ittipiboon et al. reported a linearly polarized dielectric-loaded antenna with a suspended microstrip in the air to achieve wide impedance bandwidth [70,71]. Various configurations of hybrid dielectric antennas have been illustrated in Figure 2. Several designs of linearly polarized wideband [72–90] and multi-functional [91–105] hybrid dielectric resonator antennas are reported in the open

literature. Dielectric resonator-based hybrid antenna structures are the recent research trend and focused area, as they can have the combined advantages of microstrip and dielectric resonator (DR) antennas. In the following discussion, existing DR-based hybrid structures explicitly with CP-radiation techniques are reviewed comprehensively.

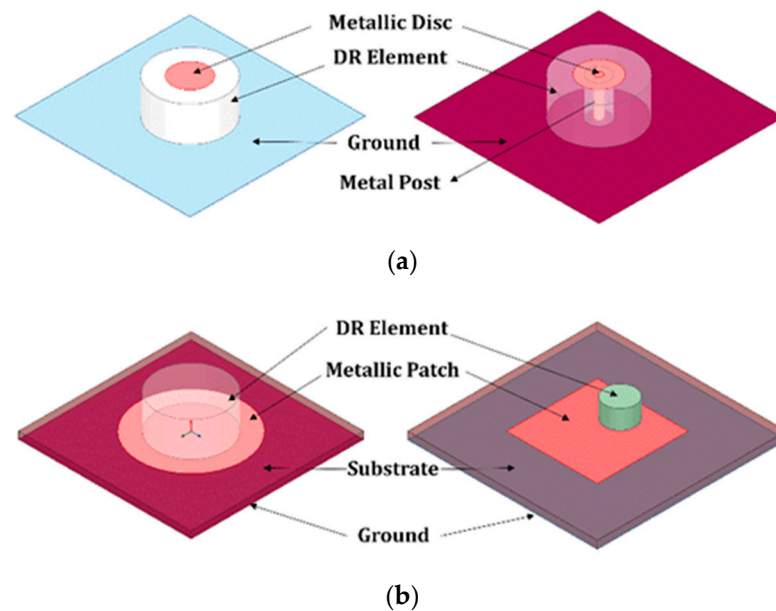


**Figure 2.** A few examples of hybrid dielectric resonator antenna technology. (a) microstrip disc loaded dielectric antennas, and (b) dielectric loaded microstrip patch antennas.

#### 4. Circularly Polarized DR Based Hybrid Antennas

##### 4.1. Wideband Hybrid Antennas with CP Radiation

Several CP radiation techniques and respective design methods have been implemented independently for microstrip and dielectric resonator antennas. However, CP radiation techniques for hybrid dielectric resonator antennas over a wide-bandwidth are challenging [106]. A compact dielectric-loaded aperture-coupled microstrip antenna is reported for L-band mobile satellite applications with CP radiation. Two dielectric-inserts [107] along the edges of the square patch are positioned for the required reduced frequency shift of 30% to the lower-side, and the cross-slot aperture creates the two-orthogonal modes desired for CP radiation with 2.5% of 3 dB AR bandwidth compared to traditional CP square patch. Similarly, four dielectric inserts [108] are used under the square patch positioned at the edges with a cross-slot feed to obtain the CP radiation. A considerable reduction of antenna size is possible by inserting dielectric blocks beneath the patch, while the desired bandwidth and the axial ratio are also achieved for L-band applications [109]. A strip-line fed compact rectangular DR-based antenna with a top-loaded rectangular patch of various aspect ratios is reported for circularly polarized radiation [110]. A suitable selection of aspect ratio for the top-loaded rectangular patch, a fundamental resonant mode of  $TE_{111}$  of the rectangular DR antenna, can be divided into two orthogonal degenerated modes ( $TE_{111}^x$  and  $TE_{111}^y$ ), which leads to circular polarization. A novel Hybrid DRA consisting of four rectangular slots on the ground-plane acts as an aperture for the DR element [111]. The wide bandwidth of 500 MHz (1130–1630 MHz) with CP radiation is achieved at boresight with a wide AR beam-width of 100 degrees. A compact Hybrid DRA composed of cylindrical DR elements and four arc-shaped slots arranged sequentially on the ground plane, which acts as an aperture to the DR is proposed [112] for GPS and GNSS applications. In this case, the CP radiation is responsible due to the geometrical arrangement of slots and the feed network with four strip-lines. A high-gain single element hybrid DRA consisting of the microstrip and the elliptic-shaped dielectric ring is proposed [113] for millimeter-wave frequency applications. The combination of microstrip and elliptical

dielectric ring is responsible for high gain and an inverted T-shaped slot is responsible for CP. The fine-tuning of the AR bandwidth and gain is possible, and can be achieved by ring-shaped DR. The maximum impedance bandwidth of 12% and an AR bandwidth of 10% with a measured gain of over 9dBi is obtained over the entire frequency band.

A modified cross-slot is concurrently acting as a radiator as well as the feeding element to the DR antenna. The resonances of modified cross-slot and DR elements are combined to form a wideband CP radiated hybrid DRA [114] with a 3 dB AR bandwidth of 24.6% (2.25–2.88 GHz) and 10 dB return-loss bandwidth of 28.6% (2.19–2.92 GHz). A hybrid structure is formed, combining a stair-shaped DR element with an open-ended slot [115] on the ground plane, which is reported for wideband CP radiation. The open-ended slot on the ground plane is responsible for a lower frequency of resonance (at 4.5 GHz) and, in turn, a wide axial-ratio bandwidth is obtained. By varying different parameters of the hybrid structure, a wide impedance bandwidth of 71.7% (3.844–8.146 GHz) and an AR band-width of 46% (4.15–6.63 GHz) is obtained. A simple feed network along with two vertical strip-lines are arranged [116] as shown in Figure 3 to produce orthogonal fields of hybrid  $HE^x_{11s}$  and  $HE^y_{11s}$  modes (presented in Figure 4) in the cylindrical DR element for wide CP radiation with AR bandwidth of 24.6% (2750–3520 MHz). The length of the vertical strip-lines along the cylindrical surface of the DRA controls the LHCP and RHCP radiation. A circularly polarized multiple inputs multiple output (MIMO) hybrid antenna [117] is formed by a parasitic patch, and the conformal strips along the sidewalls of two identical rectangular DR elements are shown in Figure 5. The single element of the proposed structure produces linear polarization at the desired frequency, and if both the elements are arranged diagonally, CP fields are created with two orthogonal modes. The AR bandwidth offered by the MIMO structure is 20.82% in the frequency band of 3.58–4.40 GHz. An electromagnetically coupled hybrid antenna comprises a hexagonal split-ring slotted hexagonal patch loaded, with a parasitic rectangular dielectric block at the radiating edge of the patch for wide-band CP radiation applications [118]. The performance analysis and features of wide-band DR-based hybrid antennas are summarized in Table 2. By considering the relative permittivity ( $\epsilon_r$ ) of the dielectric resonator in the range 9 to 80, the effective height ( $H_{eff}$ ) of hybrid DR antenna can be in the range  $0.0118\lambda < h < 0.034\lambda$ , while sustaining 10 dB RL and 3 dB AR bandwidths to the higher values. The ground plane dimensions determine the overall volume hybrid DR antenna. The size of the ground plane was chosen appropriately and not to reduce the whole volume of the antenna. The dimensions of the ground plane are kept as low as  $0.37\lambda$  in the reported literature, and it can be minimized, if the antenna designer is ready to compromise bandwidth and gain performance.

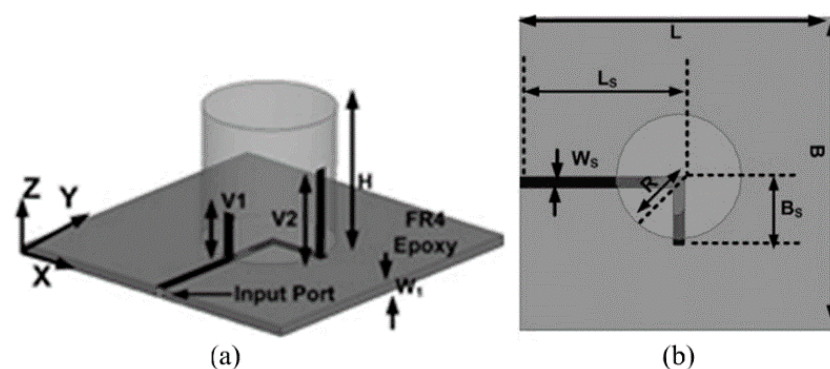
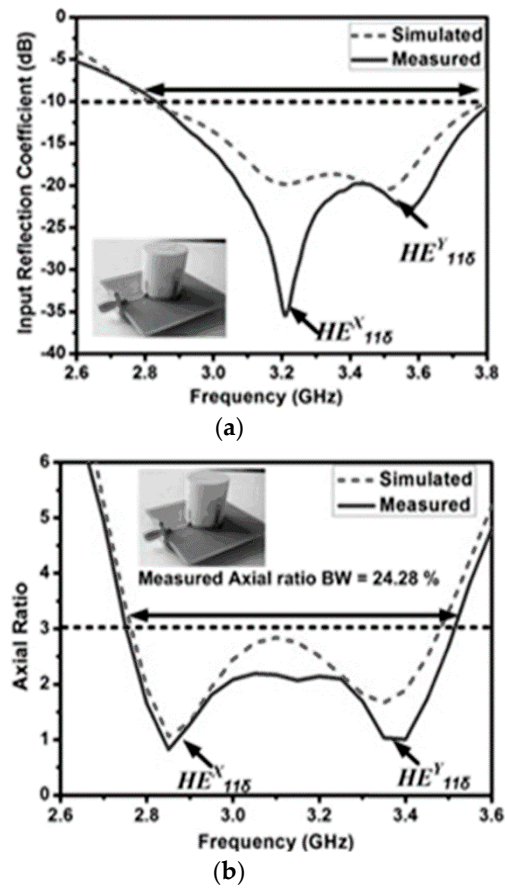
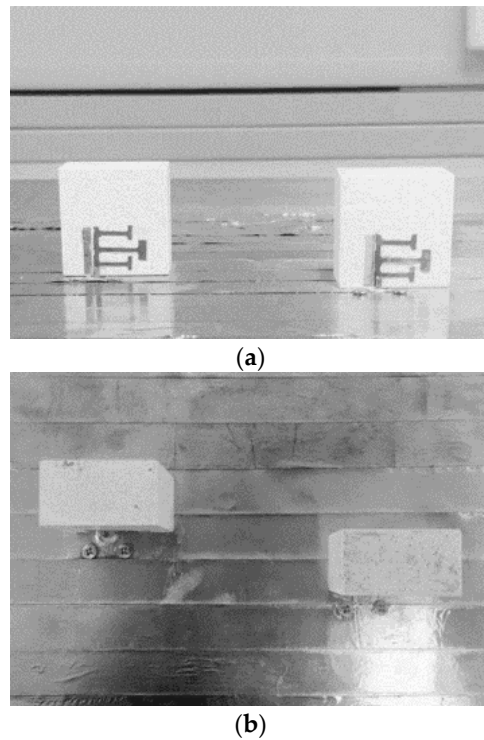


Figure 3. (a) 3D-view and (b) Top-view of hybrid structure (Reference [116]).



**Figure 4.** Representation of simulated and measured (a) S11 (b) AR plots, along with orthogonal modes. (Reference [116]).



**Figure 5.** Diagonally arranged two-element multiple inputs multiple output (MIMO) hybrid structure (a) Side view, (b) Top view (Reference [117]).



**Table 2.** Performance analysis of wideband DR-based CP hybrid antennas.

HDRA Description [Reference]	CP is Achieved by	Volume of the HDRA (in Terms of $\lambda$ at $f_r$ ) ( $L \times W \times H_{eff}$ )	$f_r$ (or) CP Bands of Resonance (GHz)	10 dB RL Bandwidth (MHz) or %	3 dB AR Bandwidth (MHz) or %	Gain (dBic)
Four dielectric inserts under the patch and coupled with cross slot [109]	Dielectric inserts and square patch coupled through cross-slot	$0.67\lambda \times 0.67\lambda \times 0.075\lambda$	L-band	7.8 %	2.5%	9.1
A strip-line fed rectangular DRA with top-loaded rectangular patch [110]	Rectangular DR element loaded with a rectangular patch with various aspect ratios	$0.37\lambda \times 0.37\lambda \times 0.048\lambda$	2170–2270	100	25 or 1.1%	3.3
Cylindrical DRA and ground plane having four slots fed through microstrip line feed network [111]	Having a feeding network consisting of four microstrip lines; wherein the four slots are constructed and geometrically arranged to ensure CP	$0.8\lambda \times 0.8\lambda \times 0.12\lambda$	1.08–1.82	740	600	5
Four sequentially rotated arc-shaped slots etched in the ground plane to feed the DRA [112]	Due to the arc-shaped slots	$0.8\lambda \times 0.8\lambda \times 0.118\lambda$	1.22–1.71	490	380	3
Aperture coupled microstrip loaded with an elliptical ring dielectric resonator [113]	A reversed T-shaped coupling slot	$6\lambda \times 4\lambda \times 0.252\lambda$	55.6–65	9400	2000	9
Rectangular DRA with modified slot and microstrip line [114]	Modified cross-slot	$0.43\lambda \times 0.43\lambda \times 0.29\lambda$	2.19–2.92	730	630	5
An open-ended slot with Stair-shaped DR loaded on the ground [115]	Combination of Stair-shaped DR and Open-ended slot on the ground plane with an offset feed	$0.46\lambda \times 0.46\lambda \times 0.07\lambda$	3.844–8.146	4302	2480	3.9
Cylindrical DR loaded on L shaped microstrip line with vertical strips-lines attached to DR [116]	Dual vertical microstrip lines with L-shaped microstrip-line arranged perpendicularly to excite orthogonal modes	$0.59\lambda \times 0.59\lambda \times 0.26\lambda$	2.82–3.83	1010	770	5.5
A rectangular DRA with conformal metal strip [117]	Employment of parasitic patch at an optimized distance beside the conformal metal strip of the two identical rectangular DRAs to generate CP	$0.46\lambda \times 0.46\lambda \times 0.34\lambda$	3.50–4.95	1450	820	6.2

#### 4.2. Multi-Functional Hybrid Antennas with CP Radiation

A combination of ring-shaped microstrip and cylindrical DR elements has been designed for dual functional applications. In this particular configuration, an independently operated microstrip-based annular ring and cylindrical dielectric resonators are used to form a hybrid structure [119], to produce dual CP-radiated bands at 4.2 GHz and 6.4 GHz, respectively, with the return-loss bandwidth higher than 6% at each band. By short-circuiting the annular ring to the ground, the perturbation of radiation patterns can be avoided after assembling both the resonators significantly. However, the shift in the resonant frequency due to the short circuit can be adjusted by modifying the annular ring dimensions. A dual CP hybrid DR antenna is formed [120] by introducing a zonal slot cut on a conducting-cavity, along with a DR element. The lower and upper bands are achieved by zonal slot and DR elements positioned on the side-wall and top of the cavity wall. An L-shaped probe is used to feed the zonal slot antenna in the cavity and

an indirect cross-coupling slot is incorporated to feed the DR element. Two even cuts are introduced to achieve CP radiation fields, and another cut is introduced in the zonal slot to obtain the desired AR. Regular unequal lengths of cross-slots under the DR element introduces another perpendicular degenerated mode for CP fields. A cross-slot is used as an aperture feed and as a radiator to produce dual-CP-bands [121]. A combination of dual-C-shaped microstrips and two DR elements are arranged in a Z-shape, forming a hybrid structure [122] to achieve multi-functional bands with CP radiation. Five bands, including one CP band, are produced in the 1 to 9 GHz frequency range. The  $TE_{01\delta}$  mode is produced due to a dual C-shaped patch and an equipoised top and bottom cylindrical DR elements responsible for orthogonal fields result in CP radiation. The performance characteristics of multi-functional DR-based hybrid antennas are presented comprehensively in Table 3. The feed, a combination of radiating elements in the hybrid structure and placement and orientation of the DR element is responsible for producing multi-functional resonant bands. As reported in Table 3, the gain in all functional bands depends on the appropriate dimension of the ground plane and the effective height of the hybrid DR antenna.

**Table 3.** Performance analysis of multi-functional DR-based CP hybrid antennas.

HDRA Description [Reference]	CP is Achieved by	Volume of the HDRA (in Terms of $\lambda$ at Lower $f_r$ ) ( $L \times W \times H_{eff}$ )	$f_r$ or CP Bands of Resonance (GHz)	10 dB RL Bandwidth (MHz)	3 dB AR Bandwidth (MHz)	Gain (dBi)
A zonal-slot antenna cut onto a conducting cavity is combined with rectangular DRA [120]	Zonal and cross slots with L-Probe feed ensures CP	$0.275\lambda \times 0.275\lambda \times 0.26\lambda$	2.34–2.53, and 4.46–5.34	190, and 880	80, and 180	5.80 and 4.29
A cross-slot acts as both the feeding structure of the DRA and an effective radiator [121]	Cross slot as aperture coupled feed and radiator	$0.475\lambda \times 0.475\lambda \times 0.098\lambda$	1.80–2.07, and 2.57–2.92	270, and 350	60, and 100	4.7, and 5.6
Consists of a Z-shaped CDRA along with a dual C-shaped patch [122]	Offset between upper and lower CDRA is responsible for CP	$0.22\lambda \times 0.22\lambda \times 0.049\lambda$	7.2–8.5	1300	500	2.5, 3.2, 3.5, 4 and 6

#### 4.3. Dual-Sense Polarized Hybrid Antennas

Earlier, a combination of monopole and ring DR antennas are ensembled to produce wide bandwidth with Omni-directional patterns [123–125]. Similar designs can also have multiple bands with orthogonal polarizations with coax-feed and dual-feed techniques, respectively. Later, a few more hybrid antennas with a combination of microstrip and DR elements are proposed for multi-functional dual-sense polarizations, which include: a circular-ring patch with a reversed L-strip [126]; an irregular square-ring patch loaded DR element [127]; a tapered microstrip line feed; modified unequal sides of hexagonal DR loaded with the square ring [128] (shown in Figure 6); an L-shaped line stub feed incorporated in an irregular rectangular slot [129]; and a line feed hybrid DR antenna [130] with top-loaded inter-digital structure. The performance characteristics of dual-sense polarized DR-based hybrid antennas are summarized in Table 4. The combination of feeding mechanism and patch design beneath or on top of the DR element, and the shape of the DR element are responsible for multi-sense polarized radiations.

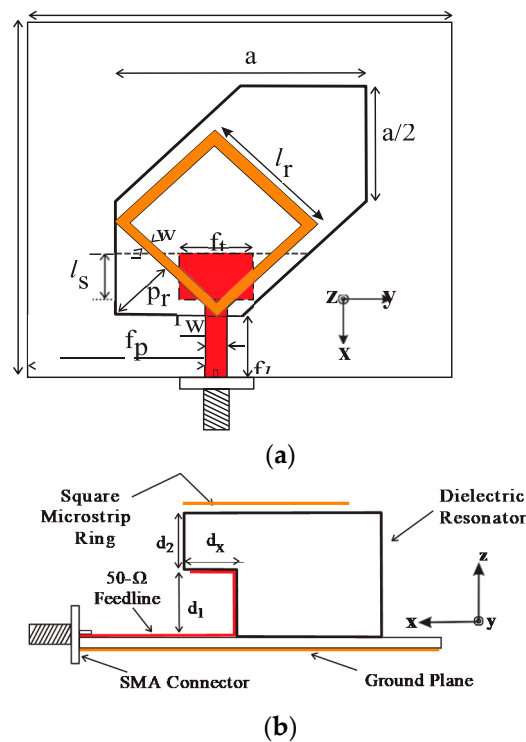


**Figure 6.** Configuration of dual-sense polarized hybrid DRA. (a) Top view, and (b) side view (Reference [128]).

**Table 4.** Performance analysis of dual-sense polarized DR-based hybrid antennas.

HDRA Description [Reference]	Volume of the HDRA (in Terms of $\lambda$ at Lower $f_r$ ) ( $L \times W \times H_{\text{eff}}$ )	Dual-Sense Polarized Bands	$f_r$ (GHz) or CP Band of Resonance	10 dB RL Bandwidth (MHz)	3 dB AR Bandwidth (MHz)	Gain (dBi)
A ring-shaped patch along with an inverted L-strip and cylindrical DRA [126]	$0.475\lambda \times 0.475\lambda \times 0.098\lambda$	LP and CP	2.9–3.93	1030	250	4
Comprises of an asymmetrical square ring-shaped printed line and a rectangular DR. The square ring is responsible for creating dual-sense radiation [127]	$0.68\lambda \times 0.57\lambda \times 0.11\lambda$	LHCP and RHCP	3.28–5.78	2500	470 and 300	3.1
Modified hexagonal DR is top-loaded with a square microstrip ring [128]	$0.44\lambda \times 0.51\lambda \times 0.152\lambda$	LHCP and RHCP	1.75–2.03, 2.23–2.96, and 3.65–3.76	280, 730 and 110	70, 150 and 80	5, 5.28 and 2.36
The asymmetric-slot radiator is fed by an L-shaped stub with the CPW line combined with rectangular-DR. Dual sense CP is obtained using a rectangular-DR over asymmetric rectangular-slot radiator with an L-shaped feed line [129]	$0.446\lambda \times 0.446\lambda \times 0.149\lambda$	LHCP and RHCP	1.75–2.73	980	860	5.5

## 5. Formulation to Find Resonance of Various Modes Associated with Hybrid DRAs

In this section, a summary of empirical formulas used in the literature to find the fundamental mode of resonant frequency and various hybrid modes for hybrid rectangular and cylindrical DRAs are given in Equations (6)–(16).

For hybrid rectangular DRA [131], the analytical solution of fundamental resonance is given in Equations (6)–(8).

$$f_{res} = \frac{C}{2\pi\sqrt{\epsilon_{r, RDR}}} \sqrt{k_x^2 + k_y^2 + k_z^2} \quad (6)$$

$$\frac{k_x a}{2} = \tan^{-1} \sqrt{\left(1 - \frac{1}{\epsilon_{r, RDR}}\right) \left(\frac{k_0}{k_x}\right)^2 - 1} \quad (7)$$

$$k_0 = \frac{2\pi}{\lambda_0} = \frac{2\pi f_{res}}{C}, \quad k_y = \frac{m\pi}{b}, \quad k_z = \frac{n\pi}{2d} \quad (8)$$

The “ $a$ ”, “ $b$ ”, and “ $d$ ” are the dimensions of the rectangular DRA designated as length, width, and height, respectively. Similarly, to find the resonant hybrid (TE<sub>01 $\delta$</sub>  and HE<sub>11 $\delta$</sub> ) modes in hybrid cylindrical DRA, the following Equations (9) and (10), respectively, are used along with the effective permittivity and height Equations (11) and (12).

$$f_{r, TE_{01\delta}} = \frac{2.327c}{2\pi d \sqrt{\epsilon_{r,eff} + 1}} \left[ 1.0 + 0.2123 \frac{d}{H_{eff}} - 0.00898 \left(\frac{d}{H_{eff}}\right)^2 \right] \quad (9)$$

$$f_{r, HE_{11\delta}} = \frac{6.321c}{2\pi d \sqrt{\epsilon_{r,eff} + 2}} \left[ 0.27 + 0.36 \frac{d}{2H_{eff}} + 0.02 \left(\frac{d}{2H_{eff}}\right)^2 \right] \quad (10)$$

If a multi-segmented antenna is considered, the resonance frequency will be affected by the layers of the substrate ( $H_S$ ) and dielectric ( $H_D$ ) materials. Accordingly, the effective height ( $H_{eff}$ ), and permittivity ( $\epsilon_{r,eff}$ ) [132,133] of the hybrid CDRA are calculated by Equations (11) and (12):

$$H_{eff} = H_{DR} + H_{Sub} \quad (11)$$

Similarly, the effective relative permittivity  $\epsilon_{r,eff}$  in Equation (8) is given by:

$$\epsilon_{r,eff} = \frac{H_{eff}}{\frac{H_{DR}}{\epsilon_{r,CDRA}} + \frac{H_{Sub}}{\epsilon_{r,sub}}} \quad (12)$$

where “ $d$ ” ( $D/2$ ) is the radius of the cylindrical DR element.

The mathematical prediction of other hybrid radiating modes has been discussed qualitatively in [134], and they are calculated by Equations (13)–(16). The higher-order modes of HEM<sub>11 $\delta$</sub>  mode are HEM<sub>11 $\delta$ +1</sub> and HEM<sub>13 $\delta$</sub> . In the case of a cylindrical structure, the predicted resonant frequencies for these higher-order modes are given by the first-order Bessel function [135] and given by Equations (13) and (14). Guha et al. proposed [136] a new hybrid mode of HEM<sub>12 $\delta$</sub>  (Equation (15)) and predicted the resonance using HEM<sub>11 $\delta$</sub>  mode and aspect ratio of CDRA. The higher order mode of HEM<sub>12 $\delta$</sub>  is HEM<sub>14 $\delta$</sub> , and it is given in Equation (16).

$$f_{r, HEM_{11\delta+1}} = 1.25 \times f_{r, HEM_{11\delta}} \quad (13)$$

$$f_{r, HEM_{13\delta}} = 1.5 \times f_{r, HEM_{11\delta+1}} + (f_{r, HEM_{11\delta+1}} - f_{r, HEM_{11\delta}}) \quad (14)$$

$$f_{r, HEM_{12\delta}} = 1.8 \times f_{r, HEM_{11\delta}} \quad (15)$$

$$f_{r, HEM_{14\delta}} = 1.25 \times f_{r, HEM_{12\delta}} \quad (16)$$

## 6. Future Scope and Challenges

Based on the review, several techniques that can be implemented in the future are listed below to achieve wideband, multi-band, high gain, and circularly polarized hybrid DR-based antennas.

- Employing metamaterial concepts and magnetic LC resonators on the metallic patch, considering dielectric-loaded patch and metallic patch loaded on top of dielectric antennas.
- Various available fractal concepts can be employed on the patch as well as the DR elements particularly to achieve multifunctional bands of resonance.
- Existing bandwidth and gain enhancement techniques can be applied for the combined form of hybrid DR-based antennas.
- A combination of a metallic waveguide, microstrip, and DR antennas with a proper feeding mechanism can be developed for future radar applications.

Implementing multi-functional CP bands is a challenge for hybrid dielectric resonator antennas with desired gain over all the resonances.

## 7. Conclusions

A brief study and evolution of circularly polarized DR-based hybrid antennas and design challenges are discussed in this article. Various methodologies and insights into obtaining wide bands and multi-functional bands with CP radiation using DR-based hybrid antennas are addressed and reviewed. A perspective analysis and study of DR antennas with various CP radiation methods are presented. The empirical formulas that are being used and correlated in the open literature to identify different resonant modes, including the fundamental mode of resonance, are addressed in the process of designing various hybrid DR antennas. Table 1 presents the past review highlights and state-of-the-art in DR antennas. Tables 2–4 present the various methods of CP radiation in designing wideband, multi-band, and dual sense polarized DR-based hybrid antennas. Based on this review, a new line of work is highlighted with important future challenges and possibilities. The qualitative and quantitative information given in this review article is useful for engineers who are working on circularly polarized wideband and multiband hybrid DRAs.

**Author Contributions:** Conceptualization, R.N. and N.K.D.; Methodology, R.N., and N.K.D.; Validation, R.K., C.-W.P., and R.R.R.; Formal Analysis, N.K.D. and R.K.; Investigation, R.N.; Resources, R.K. and C.-W.P.; Data Curation, R.N., and N.K.D.; Writing—Original Draft Preparation, R.N. and N.K.D.; Writing—Review & Editing, R.K. and C.-W.P. and R.R.R.; Visualization, R.R.R.; Supervision, R.K. and C.-W.P. All authors have read and agreed to the published version of the manuscript.

**Funding:** This research received no external funding.

**Institutional Review Board Statement:** Not applicable.

**Informed Consent Statement:** Not applicable.

**Data Availability Statement:** Not applicable.

**Conflicts of Interest:** The authors declare no conflict of interest.

## References

1. Balanis, C.A. *Antenna Theory: Analysis and Design*; Wiley: New York, NY, USA, 1982.
2. Kraus, J. Antennas since Hertz and Marconi. *IEEE Trans. Antennas Propag.* **1985**, *33*, 131–137. [[CrossRef](#)]
3. Deschamps, G.A. Microstrip Microwave Antennas. In Proceedings of the 3rd Symposium on the USAF Antenna Research and Development Program, University of Illinois, Monticello, IL, USA, 18–22 October 1953.
4. Munson, R.E. Single Slot Cavity Antennas Assembly. U.S. Patent No. 3713162, 23 January 1973.
5. Munson, R. Conformal microstrip antennas and microstrip phased arrays. *IRE Trans. Antennas Propag.* **1974**, *22*, 74–78. [[CrossRef](#)]
6. Howell, J.Q. Microstrip Antennas. *IEEE Trans. Ant. Prop.* **1975**, *AP-23*, 90–93. [[CrossRef](#)]
7. Bahl, I.J.; Bhartia, P. *Microstrip Antennas*; Artech House: Dedham, MA, USA, 1980.
8. Carver, K.R.; Mink, J. Microstrip antenna technology. *IRE Trans. Antennas Propag.* **1981**, *29*, 2–24. [[CrossRef](#)]
9. Mailloux, R.; McIlvanna, J.; Kernweis, N. Microstrip array technology. *IRE Trans. Antennas Propag.* **1981**, *29*, 25–37. [[CrossRef](#)]
10. James, J.; Hall, P.; Wood, C.; Henderson, A. Some recent developments in microstrip antenna design. *IRE Trans. Antennas Propag.* **1981**, *29*, 124–128. [[CrossRef](#)]
11. Guha, D.; Kumar, C. Microstrip Patch versus Dielectric Resonator Antenna Bearing all Commonly used Feeds: An Experimental Study to Choose the Right Element. *IEEE Ant. Prop. Mag.* **2016**, *58*, 45–55. [[CrossRef](#)]
12. Richtmyer, R.D. Dielectric Resonators. *J. Appl. Phys.* **1939**, *10*, 391–398. [[CrossRef](#)]

13. Gastine, M.; Courtois, L.; Dormann, J. Electromagnetic resonances of free dielectric spheres. *IEEE Trans. Microw. Theory Tech.* **1967**, *15*, 694–700. [[CrossRef](#)]
14. Sager, O.; Tisi, F. On Eigen Modes and Forced Resonance-Modes of Dielectric Spheres. *Proc. IEEE* **1968**, *56*, 1593–1594. [[CrossRef](#)]
15. McAllister, M.W.; Long, S.A.; Conway, G.L. Rectangular dielectric resonator antenna. *Electron. Lett.* **1983**, *19*, 218–219. [[CrossRef](#)]
16. Long, S.; McAllister, M.; Shen, L. The resonant cylindrical dielectric cavity antenna. *IRE Trans. Antennas Propag.* **1983**, *31*, 406–412. [[CrossRef](#)]
17. McAllister, M.W.; Long, S.A. Resonant hemispherical dielectric antenna. *Electron. Lett.* **1984**, *20*, 657. [[CrossRef](#)]
18. Ittipiboon, A.; Cuhaci, M.; Mongia, R.; Bhartia, P.; Antar, Y. Aperture fed rectangular and triangular dielectric resonators for use as magnetic dipole antennas. *Electron. Lett.* **1993**, *29*, 2001. [[CrossRef](#)]
19. Leung, K.W.; Luk, K.M.; Yung, E. Spherical cap dielectric resonator antenna using aperture coupling. *Electron. Lett.* **1994**, *30*, 1366–1367. [[CrossRef](#)]
20. Mongia, R.K.; Ittipiboon, A.; Bhartia, P.; Cuhaci, M. Electric-Monopole Antenna Using a Dielectric Ring Resonator. *Electron. Lett.* **1993**, *29*, 1530–1531. [[CrossRef](#)]
21. Runa, K.; Behera, S.K. Mushroom-Shaped Dielectric Resonator Antenna for WiMAX Applications. *Microw. Opt. Tech. Lett.* **2013**, *55*, 1360–1365.
22. Mongia, R.K.; Bhartia, P. Dielectric Resonator Antennas—A Review and General Design Relations for Resonant Frequency and Bandwidth. *Int. J. Microw. Millim. Wave Comput. Aided Eng.* **1994**, *4*, 230–247. [[CrossRef](#)]
23. Rao, Q.; Denidni, T.A. Study of Broadband Dielectric Resonator Antennas. *PIERS Online* **2005**, *1*, 137–141. [[CrossRef](#)]
24. Guha, D.; Antar, Y.M.M. Ultra-Wideband Monopole-Dielectric Resonator Antennas: Designs and Advances. In Proceedings of the 2010 URSI International Symposium on Electromagnetic Theory, Berlin, Germany, 16–19 August 2010; IEEE: New York, NY, USA; pp. 428–431.
25. Petosa, A.; Ittipiboon, A. Dielectric Resonator Antennas: A Historical Review and the Current State of the Art. *IEEE Antennas Propag. Mag.* **2010**, *52*, 91–116. [[CrossRef](#)]
26. Leung, K.W.; Lim, E.H.; Fang, X.S. Dielectric Resonator Antennas: From the Basic to the Aesthetic. *Proc. IEEE* **2012**, *100*, 2181–2193. [[CrossRef](#)]
27. Soren, D.; Ghatak, R.; Mishra, R.K.; Poddar, D.R. Dielectric Resonator Antennas: Designs and Advances. *Prog. Electromagn. Res. B* **2014**, *60*, 195–213. [[CrossRef](#)]
28. Kumari, R.; Gangwar, R.K. Circularly Polarized Dielectric Resonator Antennas: Design and Developments. *Wirel. Pers. Commun.* **2015**, *86*, 851–886. [[CrossRef](#)]
29. Dash, S.K.K.; Khan, T.; De, A. Modelling of dielectric resonator antennas using numerical methods: A review. *J. Microw. Power Electromagn. Energy* **2016**, *50*, 269–293. [[CrossRef](#)]
30. Dash, S.K.K.; Khan, T.; De, A. Dielectric resonator antennas: An application oriented survey. *Int. J. RF Microw. Comput. Eng.* **2016**, *27*, e21069. [[CrossRef](#)]
31. Ullah, U.; Ain, M.F.; Ahmad, Z.A. A review of wideband circularly polarized dielectric resonator antennas. *China Commun.* **2017**, *14*, 65–79. [[CrossRef](#)]
32. Dash, S.K.K.; Khan, T. Recent developments in bandwidth improvement of dielectric resonator antennas. *Int. J. RF Microw. Comput. Eng.* **2019**, *29*, e21701. [[CrossRef](#)]
33. Banerjee, U.; Karmakar, A.; Saha, A. A review on circularly polarized antennas, trends and advances. *Int. J. Microw. Wirel. Technol.* **2020**, *12*, 922–943. [[CrossRef](#)]
34. Mongia, R.K.; Ittipiboon, A.; Cuhaci, M.; Roscoe, D. Circularly Polarized Dielectric Resonator Antenna. *Electron. Lett.* **1994**, *30*, 1361–1362. [[CrossRef](#)]
35. Kishk, A.A. An elliptic dielectric resonator antenna designed for elliptic polarization with single feed. *Microw. Opt. Technol. Lett.* **2003**, *37*, 454–456. [[CrossRef](#)]
36. Li, B.; Leung, K.W. Strip-fed rectangular dielectric resonator antennas with/without a parasitic patch. *IEEE Trans. Antennas Propag.* **2005**, *53*, 2200–2207. [[CrossRef](#)]
37. Chu, L.C.Y.; Guha, D.; Antar, Y.M.M. Comb-Shaped Circularly Polarized Dielectric Resonator Antenna. *Electron. Lett.* **2006**, *42*, 785–787. [[CrossRef](#)]
38. Khoo, K.-W.; Guo, Y.-X.; Ong, L.C. Wideband Circularly Polarized Dielectric Resonator Antenna. *IEEE Trans. Antennas Propag.* **2007**, *55*, 1929–1932. [[CrossRef](#)]
39. Mohsen, K.; Kamarudin, M.R.; Mokayef, M.; Danesh, S.; Ghahferokhi, S.E.A. A New Wideband Circularly Polarized Dielectric Resonator Antenna. *Radioeng. J.* **2014**, *23*, 175–180.
40. Patel, P.; Mukherjee, B.; Mukherjee, J. A Compact Wideband Rectangular Dielectric Resonator Antenna using Perforations and Edge Grounding. *IEEE Antennas Wirel. Propag. Lett.* **2014**, *14*, 490–493. [[CrossRef](#)]
41. Majeed, A.H.; Abdullah, A.S.; Elmegri, F.; Sayidmarie, K.H.; Abd-Alhameed, R.A.; Noras, J.M. Dual-Segment S-shaped Aperture-Coupled Cylindrical Dielectric Resonator Antenna for X-band Applications. *IET Microw. Ant. Prop.* **2015**, *9*, 1673–1682. [[CrossRef](#)]
42. Trinh-Van, S.; Yang, Y.; Lee, K.-Y.; Hwang, K.C. A Wideband Circularly Polarized Pixelated Dielectric Resonator Antenna. *Sensors* **2016**, *16*, 1349. [[CrossRef](#)]
43. Rajkishor, K.; Raghvendra, K.C. A Wideband Circularly Polarized Dielectric Resonator Antenna Excited with Conformal-Strip and Inverted L-Shaped Microstrip Feed line for WLAN/WiMAX Applications. *Microw. Opt. Tech. Lett.* **2016**, *58*. [[CrossRef](#)]

44. Darimireddy, N.K.; Reddy, R.R.; Prasad, A.M. Tri-Band and Quad-Band Dual L-Slot Coupled Circularly Polarized Dielectric Resonator Antennas. *Int. J. RF Microw. Comput. Aided Eng.* **2018**, *28*, e21409. [[CrossRef](#)]
45. Sun, Y.-X.; Leung, K.W.; Mao, J.-F. Dual-Function Dielectric Resonator as Antenna and Phase-Delay-Line Load: Designs of Compact Circularly Polarized/Differential Antennas. *IEEE Trans. Antennas Propag.* **2017**, *66*, 414–419. [[CrossRef](#)]
46. Sethares, J.; Naumann, S. Design of Microwave Dielectric Resonators. *IEEE Trans. Microw. Theory Tech.* **1966**, *14*, 2–7. [[CrossRef](#)]
47. Guillon, P.; Garault, Y. Accurate Resonant Frequencies of Dielectric Resonators. *IEEE Trans. Microw. Theory Tech.* **1977**, *25*, 916–922. [[CrossRef](#)]
48. Legier, J.F.; Kennis, P.; Toutian, S.; Citeme, J. Resonant Frequencies of Rectangular Dielectric Resonators. *IEEE Trans. Microw. Theory Tech.* **1980**, *28*, 1031–1034. [[CrossRef](#)]
49. Singh, D.; Morgan, G. Technical memorandum higher mode resonances of high permittivity square cuboid dielectric resonators on integrated circuit substrates. *IEE Proc. H Microw. Antennas Propag.* **1987**, *134*, 563–565. [[CrossRef](#)]
50. Mongia, R.K.; Ittipiboon, A.; Cuhaci, M.; Roscoe, D. Radiation Q-factor of rectangular dielectric resonator antennas: Theory and experiment. In Proceedings of the IEEE Antennas and Propagation Society International Symposium and URSI National Radio Science Meeting, Seattle, WA, USA, 20–24 June 1994; 1994; pp. 764–767.
51. Petosa, A.; Simons, N.; Siushansian, R.; Ittipiboon, A.; Cuhaci, M. Design and Analysis of Multi-Segment Dielectric Resonator Antennas. *IEEE Trans. Antennas Propag.* **2000**, *48*, 738–742. [[CrossRef](#)]
52. Lee, M.T.; Luk, K.M.; Leung, K.W.; Leung, M.K. A small dielectric resonator antenna. *IEEE Trans. Antennas Propag.* **2002**, *50*, 1485–1487. [[CrossRef](#)]
53. Denidni, T.; Rao, Q.; Sebak, A. Multi-eccentric ring slot-fed dielectric resonator antennas for multi-frequency operations. In Proceedings of the IEEE Antennas Propagation Society International Symposium, Monterrey, QC, Canada, 5 June 2004.
54. Ittipiboon, A.; Petosa, A.; Roscoe, D.; Cuhaci, M. An investigation of a novel broadband dielectric resonator antenna. In Proceedings of the IEEE Antennas and Propagation Society International Symposium Digest, Baltimore, MA, USA, 21–26 July 1996; pp. 2038–2041.
55. Leung, K.; Luk, K.; Chow, K.; Yung, E. Bandwidth enhancement of dielectric resonator antenna by loading a low-profile dielectric disk of very high permittivity. *Electron. Lett.* **1997**, *33*, 725. [[CrossRef](#)]
56. Chair, R.; Kishk, A.; Lee, K.; Smith, C. Broadband aperture coupled flipped staired pyramid and conical dielectric resonator antennas. In Proceedings of the IEEE Antennas and Propagation Society Symposium, Monterrey, QC, Canada, 20–24 June 2004.
57. George, J.; Aanandan, C.K.; Mohanan, P.; Nair, K.G.; Sreemoolanadhan, H.; Sebastian, M.T. Dielectric Resonator Loaded Microstrip Antenna for Enhanced Impedance Bandwidth and Efficiency. *Microw. Opt. Technol. Lett.* **1993**, *17*, 205–207. [[CrossRef](#)]
58. Lda, I.; Sato, J.; Yoshimura, H.; Lto, K. Improvement in the Efficiency-Bandwidth Product in Small Dielectric-Loaded Antennas. *Electron. Lett.* **2000**, *36*, 861–862.
59. Bijumon, P.V.; Menon, S.K.; Sebastian, M.T.; Mohanan, P. Enhanced bandwidth microstrip patch antennas loaded with high permittivity dielectric resonators. *Microw. Opt. Technol. Lett.* **2002**, *35*, 327–330. [[CrossRef](#)]
60. Gupta, V.; Sinha, S.; Koul, S.K.; Bhat, B. Wideband dielectric resonator-loaded suspended microstrip patch antennas. *Microw. Opt. Technol. Lett.* **2003**, *37*, 300–302. [[CrossRef](#)]
61. Lapiere, M.; Antar, Y.; Ittipiboon, A.; Petosa, A. A wideband monopole antenna using dielectric resonator loading. In Proceedings of the IEEE Antennas and Propagation Society International Symposium. Digest. Held in Conjunction with: USNC/CNC/URSI North American Radio Sci. Meeting (Cat. No.03CH37450), Columbus, OH, USA, 22–27 June 2003; pp. 16–19.
62. Fan, Z.; Antar, Y.; Ittipiboon, A.; Petosa, A. Parasitic coplanar three-element dielectric resonator antenna subarray. *Electron. Lett.* **1996**, *32*, 789. [[CrossRef](#)]
63. Esselle, K.P. A Dielectric-Resonator-On-Patch (DROP) Antenna for Broadband Wireless Applications: Concept and Results. In Proceedings of the IEEE Antennas and Propagation Society International Symposium, Boston, MA, USA, 8–13 July 2001; pp. 22–25.
64. Esselle, K.P.; Bird, T.S. Hybrid Resonator Antennas for Broadband Wireless Applications. In Proceedings of the XXVIIth General Assembly of the International Union of Radio Science (URSI), Maastricht, The Netherlands, 17–24 August 2002.
65. Leung, K.W.; Wong, W.; Ng, H. Circularly polarized slot-coupled dielectric resonator antenna with a parasitic patch. *IEEE Antennas Wirel. Propag. Lett.* **2002**, *1*, 57–59. [[CrossRef](#)]
66. Mongia, R.K. Small Electric Monopole Mode Dielectric Resonator Antenna. *Electron. Lett.* **1996**, *32*, 947–949. [[CrossRef](#)]
67. Li, Z.; Wu, C.; Litva, J. Adjustable frequency dielectric resonator antenna. *Electron. Lett.* **1996**, *32*, 606. [[CrossRef](#)]
68. Ittipiboon, A.; Petosa, A.; Thirakoune, S. Bandwidth Enhancement of a Monopole using Dielectric Resonator Antenna Loading. In Proceedings of the 2002 9th International Symposium on Antenna Technology and Applied Electromagnetics ANTEM, Montreal, QC, Canada, 31 July–2 August 2002; pp. 387–390.
69. Yung, E.K.N.; Lee, W.W.S.; Luk, K.M. Microstrip antenna top-loaded by a dielectric resonator. *Microw. Opt. Technol. Lett.* **1994**, *7*, 55–57. [[CrossRef](#)]
70. Thirakoune, S.; Ittipiboon, A.; Petosa, A. Proximity-coupled patch antenna with dielectric loading. In Proceedings of the Symposium on Antenna Technology and Applied Electromagnetics [ANTEM 2000], Winnipeg, MB, Canada, 30 July–2 August 2000; pp. 231–234.
71. Ittipiboon, A.; Petosa, A.; Cuhaci, M. Dielectric Loaded Microstrip Patch Antenna. U.S. Patent No. 6,281,845, 28 August 2001.

72. Gao, Y.; Ooi, B.-L.; Ewe, W.-B.; Popov, A.P. A compact wideband hybrid dielectric resonator antenna. *IEEE Microw. Wirel. Components Lett.* **2006**, *16*, 227–229. [[CrossRef](#)]
73. Nasimuddin, N.; Esselle, K. A Low-Profile Compact Microwave Antenna with High Gain and Wide Bandwidth. *IEEE Trans. Antennas Propag.* **2007**, *55*, 1880–1883. [[CrossRef](#)]
74. Coulibaly, Y.; Denidni, T.A.; Boutayeb, H. Broadband Microstrip-Fed Dielectric Resonator Antenna for X-Band Applications. *IEEE Antennas Wirel. Propag. Lett.* **2008**, *7*, 341–345. [[CrossRef](#)]
75. Jazi, M.N.; Denidni, T.A. Design and Implementation of an Ultrawideband Hybrid Skirt Monopole Dielectric Resonator Antenna. *IEEE Antennas Wirel. Propag. Lett.* **2008**, *7*, 493–496. [[CrossRef](#)]
76. Ahmed, O.M.H.; Sebak, A.R.; Denidni, T.A. Size Reduction and Bandwidth Enhancement of a UWB Hybrid Dielectric Resonator Antenna for Short-Range Wireless Communications. *Prog. Electromagn. Res. Lett.* **2010**, *19*, 19–30. [[CrossRef](#)]
77. Ozzaim, C. Monopole Antenna Loaded by a Stepped-Radius Dielectric Ring Resonator for Ultrawide Bandwidth. *IEEE Antennas Wirel. Propag. Lett.* **2011**, *10*, 843–845. [[CrossRef](#)]
78. Denidni, T.; Weng, Z. Hybrid ultrawideband dielectric resonator antenna and band-notched designs. *IET Microw. Antennas Propag.* **2011**, *5*, 450. [[CrossRef](#)]
79. Guha, D.; Gupta, B.; Antar, Y.M.M. Hybrid Monopole-DRA's Using Hemispherical/Conical-Shaped Dielectric Ring Resonators: Improved Ultra-wideband Designs. *IEEE Trans. Antennas Propag.* **2012**, *60*, 393–398. [[CrossRef](#)]
80. Ozzaim, C.; Ustuner, F.; Tarim, N. Stacked Conical Ring Dielectric Resonator Antenna Excited by a Monopole for Improved Ultrawide Bandwidth. *IEEE Trans. Antennas Propag.* **2012**, *61*, 1435–1438. [[CrossRef](#)]
81. Wang, Y.; Liu, S.; Denidni, T.A.; Zeng, Q.; Wei, G. Integrated Ultra-Wideband Planar Monopole with Cylindrical Dielectric Resonator Antennas. *Prog. Electromagn. Res. C* **2013**, *44*, 41–53. [[CrossRef](#)]
82. Wang, Y.; Denidni, T.; Zeng, Q.; Wei, G. Design of high gain, broadband cylindrical dielectric resonator antenna. *Electron. Lett.* **2013**, *49*, 1506–1507. [[CrossRef](#)]
83. Chaudhary, R.K.; Kumar, R.; Srivastava, K.V. Wideband Ring Dielectric Resonator Antenna with Annular-Shaped Microstrip Feed. *IEEE Antennas Wirel. Propag. Lett.* **2013**, *12*, 595–598. [[CrossRef](#)]
84. Zou, M.; Pan, J. Investigation of Resonant Modes in Wideband Hybrid Omnidirectional Rectangular Dielectric Resonator Antenna. *IEEE Trans. Antennas Propag.* **2015**, *63*, 3272–3275. [[CrossRef](#)]
85. Xing, L.; Huang, Y.; Xu, Q.; Alja' Afreh, S. A Wideband Hybrid Water Antenna with an F-Shaped Monopole. *IEEE Access* **2015**, *3*, 1179–1187. [[CrossRef](#)]
86. Xing, L.; Huang, Y.; Xu, Q.; Alja' Afreh, S. Wideband, hybrid rectangular water antenna for DVB-H applications. *Microw. Opt. Technol. Lett.* **2015**, *57*, 2160–2164. [[CrossRef](#)]
87. Erfani, E.; Niroo-Jazi, M.; Tatu, S.; Denidni, T. A Hybrid Dielectric Resonator Antenna for Spectrum Sensing and Ultra-Wideband Applications. *Microw. Opt. Tech. Lett.* **2016**, *58*, 2609–2611. [[CrossRef](#)]
88. Qian, Y.-H.; Chu, Q.-X. A Broadband Hybrid Monopole-Dielectric Resonator Water Antenna. *IEEE Antennas Wirel. Propag. Lett.* **2017**, *16*, 360–363. [[CrossRef](#)]
89. Agrawal, S.; Parihar, M.S.; Kondekar, P.N. Performance Analysis of a Low-Profile Hybrid Antenna for Broadband Applications. *Wirel. Pers. Commun.* **2018**, *100*, 995–1007. [[CrossRef](#)]
90. Song, Z.; Zheng, H.; Wang, M.; Li, Y.; Song, T.; Li, E.; Li, Y. Equilateral Triangular Dielectric Resonator and Metal Patch Hybrid Antenna for UWB Application. *IEEE Access* **2019**, *7*, 119060–119068. [[CrossRef](#)]
91. Gao, Y.; Ooi, B.-L.; Popov, A.P. Dual-band hybrid dielectric resonator antenna with CPW-fed slot. *Microw. Opt. Technol. Lett.* **2005**, *48*, 170–172. [[CrossRef](#)]
92. Qinjiang, R.; Tayeb, A.D.; Sebak, A.R. A Hybrid Resonator Antenna Suitable for Wireless Communication Applications at 1.9 and 2.45 GHz. *IEEE Antennas Wirel. Propag. Lett.* **2005**, *4*, 341–343. [[CrossRef](#)]
93. Rao, Q.; Denidni, T.; Johnston, R. A novel feed for a multifrequency hybrid resonator antenna. *IEEE Microw. Wirel. Components Lett.* **2005**, *15*, 238–240. [[CrossRef](#)]
94. Ding, Y.; Leung, K.W. On the Dual-Band DRA-Slot Hybrid Antenna. *IEEE Trans. Antennas Propag.* **2009**, *57*, 624–630. [[CrossRef](#)]
95. Iellici, D.; Kingsley, S.P.; Kingsley, J.W.; O'Keefe, S.G.; Tyler, S.W.S. Hybrid Antenna Using Parasitic Excitation of Conducting Antennas by Dielectric Antennas. U.S. Patent 7,545,327, 9 June 2009.
96. Yeom, J.; Jeon, S.; Choi, H.; Kim, H. Compact Hybrid DRA Combined with PIFA. *IEICE Trans. Commun.* **2010**, *E93-B*, 2781–2783. [[CrossRef](#)]
97. Mitra, S.B.; Gupta, B. A novel multifrequency hybrid antenna. *Microw. Opt. Technol. Lett.* **2013**, *55*, 2712–2715. [[CrossRef](#)]
98. Messaoudene, I.; Denidni, T.A.; Benghalia, A. A Hybrid Integrated Ultra-Wideband/Dual-Band Antenna with High Isolation. *Int. J. Microw. Wirel. Tech.* **2015**, *8*, 341–346. [[CrossRef](#)]
99. Dhar, S.; Patra, K.; Ghatak, R.; Gupta, B.; Poddar, D.R. A Dielectric Resonator-Loaded Minkowski Fractal-Shaped Slot Loop Hepta-Band Antenna. *IEEE Trans. Antennas Propag.* **2015**, *63*, 1521–1529. [[CrossRef](#)]
100. Sahu, N.K.; Sharma, A.; Gangwar, R.K. Modified annular ring patch fed cylindrical dielectric resonator antenna for WLAN/WIMAX applications. *Microw. Opt. Technol. Lett.* **2017**, *59*, 120–125. [[CrossRef](#)]
101. Sharma, A.; Das, G.; Gangwar, R.K. Dual-band circularly polarized hybrid antenna for WLAN/WiMAX applications. *Microw. Opt. Technol. Lett.* **2017**, *59*, 2450–2457. [[CrossRef](#)]



102. Das, G.; Sharma, A.; Gangwar, R.K. Triple-Band Hybrid Antenna with Integral Isolation Mechanism for MIMO Applications. *Microw. Opt. Tech. Lett.* **2018**, *60*, 1482–1491. [[CrossRef](#)]
103. Das, G.; Sharma, A.; Gangwar, R.K. Dielectric resonator-based two-element MIMO antenna system with dual band characteristics. *IET Microw. Antennas Propag.* **2018**, *12*, 734–741. [[CrossRef](#)]
104. Anshul, G.; Ravi, K.G. Hybrid Rectangular Dielectric Resonator Antenna for Multiband Applications. *IETE Tech. Rev.* **2019**, *37*, 83–90.
105. Lin, I.K.C.; Jamaluddin, M.H.; Awang, A.; Selvaraju, R.; Dahri, M.H.; Yen, L.C.; Rahim, H.A. A Triple Band Hybrid MIMO Rectangular Dielectric Resonator Antenna for LTE Applications. *IEEE Access* **2019**, *7*, 122900–122913. [[CrossRef](#)]
106. Antar, Y.M.M.; Guha, D. Composite and Hybrid Dielectric Resonator Antennas: Recent Advances and Challenges. In Proceedings of the Twenty Third National Radio Science Conference (NRSC'2006), Menouf, Egypt, 14–16 March 2006; pp. 1–7.
107. Stout, S.M. Compact Dielectric-Loaded Patch Antennas for L-Band Mobile Satellite Applications. Master's Thesis, Carleton University, Ottawa, ON, Canada, September 1999.
108. Currie, C.J.; Antar, Y.M.M.; Petosa, A.; Ittipiboon, A. Compact Circularly Polarized Antenna Designs using Dielectrics. In Proceedings of the URSI Conference, Victoria, BC, Canada, 13–17 May 2001; pp. 359–361.
109. Currie, C.J.; Antar, Y.M.M.; Petosa, A.; Ittipiboon, A. Compact Dielectric Loaded Circularly Polarized Microstrip Antenna. *Electron. Lett.* **2001**, *37*, 1104–1105. [[CrossRef](#)]
110. Hsiao, F.-R.; Chiou, T.-W.; Wong, K.-L. Circularly Polarized Low-Profile Square Dielectric Resonator Antenna with a Loading Patch. *Microw. Opt. Technol. Lett.* **2001**, *31*, 157–159. [[CrossRef](#)]
111. Massie, G.; Caillet, M.; Clenet, M.; Antar, Y.M.M. A New Wideband Circularly Polarized Hybrid Dielectric Resonator Antenna. *IEEE Antennas Wirel. Propag. Lett.* **2010**, *9*, 347–350. [[CrossRef](#)]
112. Massie, G.; Caillet, M.; Clenet, M.; Antar, Y.M.M. Wideband Circularly Polarized Hybrid Dielectric Resonator Antenna. U.S. Patent 8,928,544, 6 January 2015.
113. Perron, A.; Denidni, T.A.; Sebak, A.R. Circularly Polarized Microstrip/Elliptical Dielectric Ring Resonator Antenna for Millimeter-Wave Applications. *IEEE Antennas Wirel. Propag. Lett.* **2010**, *9*, 783–786. [[CrossRef](#)]
114. Zou, M.; Pan, J. Wideband Hybrid Circularly Polarized Rectangular Dielectric Resonator Antenna Excited by Modified Cross-Slot. *Electron. Lett.* **2014**, *50*, 1123–1125. [[CrossRef](#)]
115. Lu, L.; Jiao, Y.-C.; Zhang, H.; Wang, R.; Li, T. Wideband Circularly Polarized Antenna with Stair-Shaped Dielectric Resonator and Open-Ended Slot Ground. *IEEE Antennas Wirel. Propag. Lett.* **2016**, *15*, 1755–1758. [[CrossRef](#)]
116. Chowdhury, R.; Mishra, N.; Sani, M.M.; Chaudhary, R.K. Analysis of a Wideband Circularly Polarized Cylindrical Dielectric Resonator Antenna with Broadside Radiation Coupled with Simple Microstrip Feeding. *IEEE Access* **2017**, *5*, 19478–19485. [[CrossRef](#)]
117. Iqbal, J.; Illahi, U.; Sulaiman, M.I.; Alam, M.M.; Su'ud, M.M.; Mohd Yasin, M.N. Mutual Coupling Reduction using Hybrid Technique in Wideband Circularly Polarized MIMO Antenna for WiMAX Applications. *IEEE Access* **2019**, *7*, 40951–40958. [[CrossRef](#)]
118. Darimireddy, N.K.; Park, C.-W. Electromagnetic Coupled Circularly Polarized Hybrid Antenna for LTE Applications. In Proceedings of the 2020 IEEE International Symposium on Antennas and Propagation and North American Radio Science Meeting, Montreal, QC, Canada, 5–10 July 2020.
119. Nannini, C.; Ribero, J.-M.; Dauvignac, J.-Y.; Pichot, C. A Dual-Frequency Circularly Polarized Structure Antenna. *Microw. Opt. Technol. Lett.* **2002**, *32*, 418–420. [[CrossRef](#)]
120. Ding, Y.; Leung, K.W.; Luk, K.M. Compact Circularly Polarized Dual-band Zonal-Slot/DRA Hybrid Antenna Without External Ground Plane. *IEEE Trans. Antennas Propag.* **2011**, *59*, 2404–2409. [[CrossRef](#)]
121. Zou, M.; Pan, J.; Zuo, L.; Nie, Z.-P. Investigation of a cross-slot-coupled dual-band circularly polarized hybrid dielectric resonator antenna. *Prog. Electromagn. Res. C* **2014**, *53*, 187–195. [[CrossRef](#)]
122. Sharma, A.; Gangwar, R.K. Circularly Polarized Hybrid Z-Shaped Cylindrical Dielectric Resonator Antenna for Multi-band Applications. *IET Microw. Antennas Propag.* **2016**, *10*, 1259–1267. [[CrossRef](#)]
123. Guha, D.; Antar, Y.M.M.; Ittipiboon, A.; Petosa, A.; Lee, D. Improved design guidelines for the ultra wideband monopole-dielectric resonator antenna. *IEEE Antennas Wirel. Propag. Lett.* **2006**, *5*, 373–376. [[CrossRef](#)]
124. Lapierre, M.; Antar, Y.; Ittipiboon, A.; Petosa, A. Ultra wideband monopole/dielectric resonator antenna. *IEEE Microw. Wirel. Components Lett.* **2005**, *15*, 7–9. [[CrossRef](#)]
125. Gray, D.; Watanabe, T. Three Orthogonal Polarization DRA-Monopole Ensemble. *Electron. Lett.* **2003**, *39*, 766–767. [[CrossRef](#)]
126. Sharma, A.; Gangwar, R.K. Triple-band dual-polarized hybrid cylindrical dielectric resonator antenna with hybrid modes excitation. *Prog. Electromagn. Res. C* **2016**, *67*, 97–105. [[CrossRef](#)]
127. Sahu, N.K.; Sharma, A.; Gangwar, R.K. Design and analysis of wideband composite antenna with dual-sense circular polarization characteristics. *Microw. Opt. Technol. Lett.* **2018**, *60*, 2048–2054. [[CrossRef](#)]
128. Altaf, A.; Seo, M. Triple-Band Dual-Sense Circularly Polarized Hybrid Dielectric Resonator Antenna. *Sensors* **2018**, *18*, 3899. [[CrossRef](#)]
129. Kumar, R.; Nasimuddin; Chaudhary, R.K. Wideband circularly polarized hybrid dielectric resonator antenna with bi-directional radiation characteristics for various wireless applications. *Int. J. RF Microw. Comput. Eng.* **2019**, *29*. [[CrossRef](#)]

130. Darimireddy, N.K.; Park, C.-W.; Reddy, R.R.; Reddy, B.R.S. Multi-Band Rectangular Hybrid Antennas Loaded with Inter-Digital Structure Slot. In Proceedings of the IEEE Indian Conference on Antennas and Propagation (IEEE-InCAP), Ahmedabad, India, 19–22 December 2019.
131. Rahim, S.B.A.; Lee, C.K.; Qing, A.; Jamaluddin, M.H. A Triple-Band Hybrid Rectangular Dielectric Resonator Antenna (RDRA) for 4G LTE Applications. *Wirel. Pers. Commun.* **2017**, *98*, 3021–3033. [[CrossRef](#)]
132. Gangwar, R.K.; Sharma, A.; Gupta, M.; Chaudhary, S. Hybrid Cylindrical Dielectric Resonator Antenna with HE 11 $\delta$  And HE 12 $\delta$  Mode Excitation for Wireless Applications. *Int. J. RF Microwav. Comput. Aided. Eng.* **2016**, *26*, 812–818. [[CrossRef](#)]
133. Kajfez, D.; Glisson, A.; James, J. Computed Modal Field Distributions of Isolated Dielectric Resonators. *IEEE Trans. Antennas Propag.* **1984**, *32*, 1609–1616.
134. Sharma, A.; Das, G.; Gupta, S.; Gangwar, R.K. Quad-Band Quad-Sense Circularly Polarized Dielectric Resonator Antenna for GPS/CNSS/WLAN/WiMAX Applications. *IEEE Antennas Wirel. Propag. Lett.* **2020**, *19*, 403–407. [[CrossRef](#)]
135. Garg, R.; Bhartia, P.; Bahl, I.; Ittipiboon, A. *Microstrip Antenna Design Handbook*; Artech House: Norwood, MA, USA, 2001.
136. Guha, D.; Gupta, P.; Kumar, C. Dualband cylindrical dielectric resonator antenna employing HEM11 $\delta$  and HEM12 $\delta$  modes excited by new composite aperture. *IEEE Trans. Antennas Propag.* **2015**, *63*, 433–438. [[CrossRef](#)]